Plasmodium infection downregulates hypoxia-inducible factor 1α expression to suppress the vascularization and tumorigenesis of liver cancer

RUNLING WU[1*], XIAO CHEN[2*], HUAN CHEN[3], MEI LI[4] and YUN LIANG[3]

[1]Department of Geriatric Respiratory Medicine, The First Affiliated Hospital of Kunming Medical University, Kunming, Yunnan 650032, P.R. China; [2]Department of Medical Oncology, The First Affiliated Hospital of Kunming Medical University, Kunming, Yunnan 650032, P.R. China; [3]Department of Hepatobiliary Surgery, The First Affiliated Hospital of Kunming Medical University, Kunming, Yunnan 650032, P.R. China; [4]Department of Clinical Medicine, The First Affiliated Hospital of Kunming Medical University, Kunming, Yunnan 650032, P.R. China

Received May 17, 2024; Accepted September 6, 2024

DOI: 10.3892/ol.2024.14737

Abstract. Liver cancer is characterized by hypervascularization. Anti-angiogenic agents may normalize the tumor vasculature and improve the efficacy of other treatments. The present study aims to investigate the anti-angiogenic effect of *Plasmodium* infection in a mouse model of implanted liver cancer cells. HepG2 cells were injected into the left liver lobe of nude mice as a model of *in situ* hepatic tumorigenesis. *Plasmodium yoelii* parasitized erythrocytes were administered in the animal model of liver cancer to introduce *Plasmodium* infection. The tumor growth and microvascular density were determined in the presence or absence of *Plasmodium* infection. The expression levels of hypoxia-inducible factor 1α (HIF-1α) and angiogenesis-related factors were evaluated using western blotting and reverse transcription-quantitative PCR analysis. The results demonstrated that *Plasmodium* infection suppressed tumor growth and vascularization in the mouse model of implanted HepG2 cells. *Plasmodium* parasites reduced the expression of pro-angiogenic factors (vascular endothelial growth factor A and angiopoietin 2), matrix metalloproteinases [(MMP)2 and MMP9] and inflammatory cytokines [tumor necrosis factor α, interleukin 6 (IL)-6) and IL-1β] in both hepatic and tumor tissues. HIF-1α was downregulated in both hepatic and tumor tissues upon *Plasmodium* infection, and HIF-1α overexpression rescued angiogenesis and tumor growth under the condition of *Plasmodium* infection. In conclusion, the results of the present study demonstrated the anti-angiogenic and anti-tumorigenic effects of *Plasmodium* infection on liver cancer through downregulating HIF-1α expression, indicating that *Plasmodium* parasites could be developed as an intervention strategy to restrain neo-angiogenesis in liver cancer.

Correspondence to: Dr Yun Liang, Department of Hepatobiliary Surgery, The First Affiliated Hospital of Kunming Medical University, 295 Xichang Road, Wuhua, Kunming, Yunnan 650032, P.R. China
E-mail: liangyun132001@163.com

*Contributed equally

Key words: liver cancer, *Plasmodium*, angiogenesis, hypoxia-inducible factor 1α, CD31

Introduction

Liver cancer has become one of the leading malignancies worldwide, with a continuous increase in annual incidence from 1990 to 2015 (1). It has been estimated that incident cases of liver cancer will exceed 1 million by 2025 (2). Hepatocellular carcinoma represents the most common form of liver cancer and comprises 75-85% of total liver cancer cases (3,4). Hepatic disorders due to unhealthy lifestyles and hepatitis B virus infection are becoming the major etiologies of liver cancer (5,6). For instance, there is an increased risk of liver cancer development in patients with non-alcoholic steatohepatitis (7). Surgical resection together with adjuvant chemotherapy remains as the mainstay of liver cancer treatment; however, postoperative recurrence and metastasis can seriously undermine the prognosis of patients with liver cancer (8). According to the World Health Organization, the recurrence rate of liver cancer at 2 years post-surgery in 2018 was as high as 61.6% (9). Currently, there is a lack of therapeutic strategies for the prevention and treatment of liver cancer metastasis (10).

Neo-angiogenesis is a key feature in the clinical progression of liver cancer. The hypervascular nature of hepatic tumors implies the significance of neo-vascularization in the pathophysiological progression of these tumors (11). Several angiogenic pathways have been found to be dysregulated in liver cancer. Tumor cells can secrete pro-angiogenic factors, including vascular endothelial growth factor A (VEGFA), angiopoietin 2 (Ang2), fibroblast growth factor 2 (FGF2) and platelet-derived growth factor A (PDGFA), which bind to receptors expressed on endothelial cells to promote

angiogenesis (12). Hypoxia has been recognized as an important factor that upregulates expression of VEGFA, FGF2 and PDGFA in tumor cells (13). Moreover, overexpression of extracellular matrix remodelers such as matrix metalloproteinases (MMP)2 and 9 can contribute to neo-angiogenesis, local tissue invasion and metastasis (14,15). Furthermore, production of inflammatory cytokines such as tumor necrosis factor (TNF)-α and interleukin (IL)-1β is also implicated in the angiogenesis and invasion of liver cancer (16-18). As hyper-vascularization facilitates tumor growth, tissue invasion and metastasis, anti-angiogenic agents have been proposed to normalize the tumor vasculature and improve the efficacy of other treatments such as chemotherapy and radiation (19).

Plasmodium is a single-cell protozoan responsible for malaria which inhabits hepatocytes to enter a dormant state, and the subsequent reproduction of merozoites leads to hepatocyte rupture (20). Accumulating evidence suggests that *Plasmodium* infection suppresses tumor growth and metastasis in a murine Lewis lung cancer model (21,22). There is also evidence that malaria incidence and cancer mortality are inversely associated (23). Furthermore, *Plasmodium* infection could curtail recurrence and metastasis of liver cancer by suppressing epithelial-mesenchymal transition (24). Although *Plasmodium* infection has been reported to inhibit angiogenesis by modulating the infiltration of tumor-associated macrophages in liver cancer (25), the effect of *Plasmodium* infection on tumor cell-derived angiogenic signaling remains unclear.

The present study established a murine model of implanted HepG2 cells and assessed the impact of *Plasmodium* infection on vascularization and tumorigenesis. HepG2 cells were injected into the left liver lobe of nude mice as a model of *in situ* hepatic tumorigenesis. *Plasmodium yoelii* parasitized erythrocytes were administered in the animal model of liver cancer to introduce *Plasmodium* infection. The tumor growth and microvascular density were determined in the presence or absence of *Plasmodium* infection. The expression levels of hypoxia-inducible factor 1α (HIF-1α) and angiogenesis-related factors were evaluated using western blotting and reverse transcription-quantitative PCR analysis.

Materials and methods

Animal model of liver cancer and Plasmodium infection. BALB/c nude mice (male; 4-5 weeks old; weight, 20-25 g; n=40 mice; n=15 for *Plasmodium propagation*; n=25 for *in situ* liver cancer model) were purchased from Shanghai Laboratory Animal Center Co., Ltd. and raised at a standard specific pathogen-free facility with a 12 h-light/dark cycle. All animal experiments described in the present study were performed in collaboration with Yunnan Bestai Biotechnology Co., Ltd., a qualified animal research facility. The animals were housed under controlled conditions with a temperature of 22±2˚C, relative humidity of 50-60% and a 12-h light/dark cycle. They had free access to standard laboratory food and water *ad libitum*. The animal protocols in the present study were approved by the Experimental Animal Ethics Committee of Yunnan Bestai Biotechnology Co (Kunming, China; approval no. BST-MICE-20221229-01).

HepG2 cells were purchased from The Cell Bank of Type Culture Collection of The Chinese Academy of Sciences, and cultured in DMEM high glucose medium containing 10% FBS (Gibco; Thermo Fisher Scientific, Inc.), 100 U/ml penicillin and 100 μg/ml streptomycin (Beyotime Institute of Biotechnology) in a humidified incubator containing 5% CO_2 at 37˚C. This cell line was authenticated by the supplier through STR profiling.

To stably express HIF-1α, HepG2 cells were infected with a lentivirus carrying the cDNA of HIF-1α (synthesized by GenScript Biotech Corporation). The empty lentiviral vector was used as a negative control. Lentivirus was prepared in 293T cells in a 10 cm dish at 70-80% confluence. 293T cells were transfected with 12 μg pLX304-HIF-1α expression plasmid and 12 μg MISSION® Lentiviral Packaging Mix (cat. no. SHP001; Sigma-Aldrich; Merck KGaA) using Lipofectamine™ 3000 transfection reagent (Invitrogen™; Thermo Fisher Scientific, Inc.) for 48 h at 37˚C. The lentivirus-containing supernatant was collected 48 h post-transfection, filtered through a 0.45 μm filter to remove cells and debris, and used to transduce HepG2 cells at an multiplicity of infection of 10 in the presence of 8 μg/ml polybrene. After 48 h, transduced HepG2 cells overexpressing HIF-1α were selected with 10 μg/ml blasticidin for 2 weeks to eliminate uninfected cells, and HIF-1α overexpression was confirmed by western blotting, as described below.

The *Plasmodium yoelii* (Py) nonlethal strain (Py17XNL) was purchased from the Malaria Research and Reference Reagent Resource Center, and propagated in 8-week old BALB/c mice (male; weight, 30-35 g; housed as aforementioned) at an initial injection dose of $5x10^5$ infected red blood cells (25). To isolate parasitized erythrocytes, blood was collected from the donor mice with >20% parasitemia via cardiac puncture under anesthesia with 240 mg/kg Avertin (1.25% Tribromoethanol) through intraperitoneal injection. Animals were euthanized after blood collection via carbon dioxide asphyxiation, followed by cervical dislocation. The blood was immediately transferred to heparinized tubes to prevent coagulation. Erythrocytes were separated from whole blood by centrifugation at 800 x g for 10 min at 4˚C. The erythrocyte pellet was washed twice with sterile PBS, resuspended in sterile saline, and counted using a hemocytometer. The blood parasitemia level in the donor mice (% red blood cells infected by the malaria parasite) was determined by examining thin blood smears with a light microscope (Olympus BX53; Olympus Corporation) at 1,000x magnification under oil immersion. Blood samples with parasitemia level >20% were used to prepare a desirable amount of parasitized erythrocytes for further infection. Based on the parasitemia level determined by the blood smear examination, the appropriate volume of erythrocyte suspension containing $5x10^5$ parasitized erythrocytes was calculated and diluted to a final volume of 100-200 μl with sterile saline for intraperitoneal injection into the recipient mice.

A total of $2x10^6$ HepG2 cells/animal were injected into the left liver lobe of nude mice as an *in situ* tumor growth model of liver cancer (26-28), after anesthetization with 240 mg/kg Avertin (1.25% Tribromoethanol) through intraperitoneal injection. A total of 7 days after tumor cell injection, the mice were intraperitoneally injected with $5x10^5$ parasitized erythrocytes

or uninfected erythrocytes (control) from the donor mice. On day 17 post-parasite injection, the mice were sacrificed for tissue collection. For euthanasia, a chamber was connected to a carbon dioxide cylinder with a flow rate to displace 40% of the cage volume/minute. Mice were placed into the euthanizing chamber for 10 min until no movement was observed. Animal death was further assured by subsequent cervical dislocation. All the animals (including the donor mice) were euthanized by the same method. A total of 15 donor BALB/c mice were used for Py propagation and erythrocyte collection. For tumor formation experiments, a total of 25 BALB/c nude mice were used, in which 5 mice were used for the initial *in situ* tumor model validation experiment. The remaining 20 mice were divided into 4 groups with 5 animals/group as follows: i) Sham (normal liver group); ii) HepG2 injection; iii) HepG2 + Py; and iv) HepG2 (HIF-1α) + Py.

Animal health and behavior were monitored daily throughout the experiment, with increased frequency to twice daily following tumor cell injection and *Plasmodium* infection. Trained personnel handled the animals to reduce stress and discomfort, and adequate anesthesia was provided for all surgical procedures. Welfare considerations included providing environmental enrichment, maintaining appropriate housing conditions, and minimizing handling stress. Animal health status was regularly monitored, and humane endpoints were established and implemented promptly, including euthanasia if animals showed signs of severe illness, significant weight loss (>20% initial body weight), a tumor size >2 cm, or any conditions causing obvious pain or distress that could not be alleviated by analgesics.

To accurately measure tumor weight, the present study used a meticulous isolation process. After harvesting the livers, visible tumor nodules were carefully excised using sterile surgical instruments. Fine dissection was then performed under a dissecting microscope to remove any remaining normal liver tissue from the tumor mass. The isolated tumor tissue was gently washed in cold PBS to remove blood and debris, then carefully blotted on sterile filter paper to remove excess fluid. Immediately after this preparation, the cleaned and dried tumor tissue was weighed using a high-precision analytical balance (ME204E; Mettler Toledo). This process was repeated for all tumor nodules in each liver, with the total weight of tumor tissue from each liver recorded for subsequent comparisons between groups.

Immunohistochemistry (IHC) of CD31. Immunohistochemical staining of CD31 was performed using 5-μm sections of formalin-fixed paraffin-embedded tumor tissues using the VENTANA BenchMark Special Stain system (Roche Diagnostics). Tissues were fixed in 10% neutral buffered formalin at 4˚C for 24 h before paraffin embedding. After deparaffinization in xylene (3 changes, 5 min each) at 60˚C and hydration through a descending ethanol series (100, 95, 80 and 70%; 5 min each), followed by washing in distilled water for 5 min, antigen retrieval was performed using a citrate unmasking solution (10X; SignalStain® Citrate Unmasking Solution; cat. no. 14746; Cell Signaling Technology, Inc.) for 10 min at a sub-boiling temperature (95-98˚C). After cooling, the sections were washed in distilled H_2O and incubated in 3% hydrogen peroxide for 10 min at 37˚C. The sections were then washed three times in TBST buffer (Tris-buffered saline with 0.1% Tween-20; 5 min each time), and blocked for 1 h at room temperature in TBST with 5% normal goat serum (Cell Signaling Technologies, Inc.). Anti-CD31 antibodies (1:100; cat. no. ab124432; Abcam) was applied to stain the sections overnight at 4˚C. After washing, the sections were incubated with 3 drops of SignalStain® Boost IHC Detection Reagent (horseradish peroxidase, rabbit; cat. no. 8114; Cell Signaling Technology, Inc.) for 30 min at room temperature. Signal development was performed using 200 μl SignalStain® DAB Substrate Kit (cat. no. 8059; Cell Signaling Technology, Inc.) for 5 min. After washing and dehydration, the sections were mounted with coverslips using mounting medium (cat. no. 14177; Cell Signaling Technology, Inc.). Images were captured under a Leica DMI6000 microscope (Leica Microsystems GmbH) at x200 magnification.

Giemsa staining. Liver tumor tissues were fixed in 4% paraformaldehyde overnight at 4˚C and then cut into 50-μm sections. Sections were treated with 3% hydrogen peroxide and 0.25% Triton X-100 in 1X TBS for 30 min. Tissue sections were then stained with the Giemsa Stain Kit (cat. no. ab150670; Abcam) at room temperature (22-25˚C) for 15 min, based on the supplier's instructions. Nuclei were counterstained with hematoxylin solution at room temperature (22-25˚C) for 15 min. Images were captured under a Leica DMI6000 microscope (Leica Microsystems GmbH).

Terminal deoxynucleotidyl transferase dUTP nick end labeling (TUNEL). Cell death events in tumor tissues were assessed using the Biotin TUNEL Staining Kit (cat. no. T2191, Beijing Solarbio Science & Technology Co., Ltd.). Tissue samples were fixed in 10% neutral buffered formalin at 4˚C for 24 h. The fixed tissues were then dehydrated and paraffin-embedded following standard histological procedures. Paraffin-embedded tumor tissues were processed into 5-μm sections. After deparaffinization in xylene (3 changes, 5 min) at 60˚C and hydration through a descending ethanol series (100, 95, 80 and 70%; 5 min), followed by washing in distilled water for 5 min,, tissue sections were incubated with 20 μg/ml Protease K at 37˚C for 15 min, followed by treatment with 3% hydrogen peroxide at room temperature for 10 min. The sections were then labeled with a working solution containing TdT enzyme, Biotin-dUTP and a Biotin labeling solution at 37˚C for 1 h. After washing with TBST buffer (Tris-buffered saline with 0.1% Tween-20; 5 min each time), the sections were incubated with a Streptavidin-horseradish peroxidase solution at room temperature for 30 min. The staining signal was developed using 0.2 ml DAB reagent at room temperature for 2-5 min. After dehydration with 95% ethanol, the sections were treated with xylene for 5 min before observation. The nuclei were then counterstained with hematoxylin (0.1% w/v) for 5 min at room temperature. After rinsing in running tap water for 5 min, sections were dehydrated through an ascending ethanol series, cleared in xylene and mounted using DPX mounting medium (Sigma-Aldrich). Stained sections were observed using an Olympus BX53 light microscope. A total of five random fields of view were examined for each section at 400x magnification.

Reverse transcription (RT)-quantitative PCR (qPCR) analysis. RNA samples were extracted from tissues using Trizol reagent (Beyotime Institution of Biotechnology). A total of 1 μg RNA sample was reverse transcribed into complementary DNA using the PrimeScript™ RT Reagent Kit (cat. no. RR037A; Takara Bio, Inc.). The reverse transcription reaction was performed under the following conditions: 37˚C for 15 min (reverse transcription), followed by 85˚C for 5 sec (inactivation of reverse transcriptase) and then cooled to 4˚C.. qPCR was performed using the 7500 Real-Time PCR System (Applied Biosystems; Thermo Fisher Scientific, Inc.) using the SYBR premix master mix (cat. no. SR1110; Beijing Solarbio Science & Technology Co., Ltd.). The PCR cycling conditions were as follows: Initial denaturation at 95˚C for 30 sec, followed by 40 cycles of denaturation at 95˚C for 5 sec and annealing/extension at 60˚C for 30 sec. Relative gene expression was determined by the $2^{-\Delta\Delta Cq}$ method (29), using β-actin as the reference gene. For human genes, the following primers were used: MMP-2, (forward) 5'-CCCTTTGACGGTAAGGAC GGACTC-3' and (reverse) 5'-GCCCTGGAAGCGGAATGG AA-3'; MMP-9, (forward) 5'-CTATGGTCCTCGCCCTGA ACCTG-3' and (reverse) 5'-AAGGCACAGTAGTGGCCG TAGAAGG-3'; IL-1β, (forward) 5'-CCGACCACCACTACA GCAAG-3' and (reverse) 5'-ATGGACCAGACATCACCA AGC-3'; IL-6, (forward) 5'-ATGTGTGAAAGCAGCAAA GAGGCAC-3' and (reverse) 5'-GTGCCTCTTTGCTGCTTT CACACAT-3'; TNF-α, (forward) 5'-CCCGAGTGACAAGCC TGTAGCC-3' and (reverse) 5'-CCCTTGAAGAGGACCTGG GAGTAGAT-3'; and β-actin, (forward) 5'-CATGTACGT TGCTATCCAGGC-3' and (reverse) 5'-CTCCTTAATGTC ACGCACGAT-3'. For mouse genes, the following primers were used: MMP-2, (forward) 5'-TCAACGGTCGGGAAT ACAGCA-3' and (reverse) 5'-CCACCCACAGTGGACATA GCG-3'; MMP-9, (forward) 5'-CGGCAACGGAGAAGGCAA AC-3' and (reverse) 5'-CGTCTATGTCGTCTTTATTCAGAG GGA-3'; IL-1β, (forward) 5'-CTCGTGCTGTCGGACCCAT-3' and (reverse) 5'-CAGGCTTGTGCTCTGCTTGTGA-3'; IL-6, (forward) 5'-TGCCTTCTTGGGACTGATG-3' and (reverse) 5'-TCTGGCTTTGTCTTTCTTGTTA-3'; TNF-α, (forward) 5'-ACTCCAGGCGGTGCCTATGTC-3' and (reverse) 5'-GCT CCTCCACTTGGTGGTTTGT-3'; and β-actin, (forward) 5'-GTGACGTTGACATCCGTAAAGA-3' and (reverse) 5'-GCCGGACTCATCGTACTCC-3'.

Western blotting. Protein sample extraction was performed using a RIPA buffer (cat. no. P0013B; Beyotime Institute of Biotechnology), supplemented with a protease inhibitor cocktail (cat. no. 78430, Thermo Fisher Scientific, Inc.) on ice for 15 min. Sample concentration was determined using a BCA assay kit (cat. no. P0012; Beyotime Institute of Biotechnology). After denaturation, 20 μg of total protein per lane was separated by 12% SDS-PAGE and then transferred onto a PVDF membrane. The membrane was probed with the following primary antibodies: anti-β-actin (1:2,000; cat. no. ab8227; Abcam), anti-HIF-1α (1:1,000; cat. no. ab51608; Abcam), anti-VEGFA (1:1,000; cat. no. ab46154; Abcam), and anti-Ang2 (1:1,000; cat. no. ab155106; Abcam) at 4˚C overnight. After washing using TBST with 5% Tween-20 buffer, horseradish peroxidase-conjugated secondary antibodies (1:2,000; ab205718; Abcam) were applied at room temperature for 1 h.

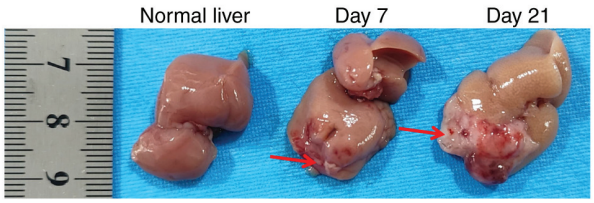

Figure 1. Intra-hepatic model of liver cancer in nude mice. HepG2 cells were injected into the liver tissues of nude mice to generate xenograft tumorigenesis. Images of liver tissues (without HepG2 injection), liver tissues at 7 days post-inoculation and liver tissues at 21 days post-inoculation were shown. Arrows indicate tumor formation.

Signals of protein bands were developed using the BeyoECL Plus Enhanced Chemiluminescence Western Blotting Substrate Kit (cat. no. P0018M; Beyotime Institute of Biotechnology). The western blot results were semi-quantified by densitometric analysis using ImageJ software (version 1.53c; National Institutes of Health).

Statistical analysis. Data are presented as mean ± standard deviation. Data analysis was performed using GraphPad Prism software (version 9.3.1; Dotmatics). Comparisons between two groups were assessed using an unpaired Student's t-test, and one-way ANOVA was used for multiple comparisons, followed by Tukey's post hoc test for pairwise comparisons. $P<0.05$ was considered to indicate a statistically significant difference.

Results

Plasmodium infection suppresses the tumorigenesis of HepG2 cells in nude mice. To assess the effect of *Plasmodium* on the tumorigenesis of liver cancer, HepG2 cells were injected into the left liver lobe of nude mice as a preliminary experiment to demonstrate *in situ* tumor formation. Liver tissues were harvested 7 and 21 days after HepG2 cell injection, with liver tissues from the non-injected normal group serving as controls. Tumor formation in liver tissues was observed 7 days post-injection, with increased *in situ* tumor growth evident 21 days post-injection (Fig. 1). A total of 7 days after tumor cell injection, the mice were intraperitoneally injected with Py parasitized erythrocytes (HepG2 + Py group) or uninfected erythrocytes (as the control: HepG2 group). On day 17 post-parasite injection, the mice were euthanized and xenograft tumors were collected for histological analysis. Giemsa staining revealed that in the HepG2 + Py group, infection of Py was associated with the deposition of hemozoin (the byproduct of hemoglobin digestion by *Plasmodium*) (20) in tumor tissues (Fig. 2A). *Plasmodium* infection also significantly suppressed tumor formation of HepG2 cells in nude mice compared with the uninfected control group (Fig. 2B and C). Furthermore, detection of apoptotic events by TUNEL staining revealed that *Plasmodium* infection was associated with a significant increase in the cell death of tumor tissues, compared with the uninfected control group (Fig. 2D).

Plasmodium infection attenuates angiogenesis in tumor and para-cancerous hepatic tissues. Vascularization in tumor tissues of each experimental group was assessed. Analysis

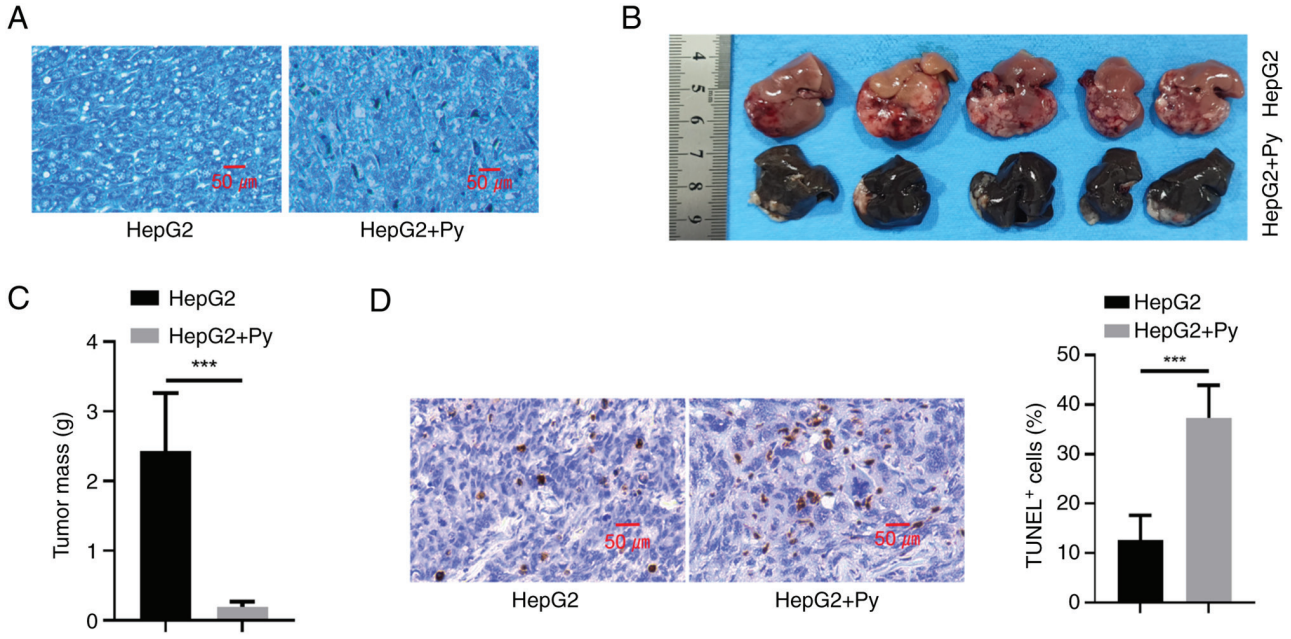

Figure 2. *Plasmodium* infection suppresses tumorigenesis of HepG2 cells in nude mice. HepG2 cells were injected into the left liver lobe of nude mice. A total of 7 days after tumor cell injection, mice were intraperitoneally injected with Py parasitized erythrocytes (HepG2 + Py group) or uninfected erythrocytes (as the control: HepG2 group). The mice were euthanized and xenograft tumors were collected on day 17 post parasite injection. (A) Giemsa staining of hemozoin (the byproduct of hemoglobin digestion by *Plasmodium*) in tumor tissues. (B) Xenograft liver tumor images in each experimental group. (C) Mass of tumors in each group. (D) Detection of apoptotic events by TUNEL staining. n=5 in each group. ***P<0.001. Py, *Plasmodium yoelii*.

of microvascular density (MVD) by IHC staining of CD31 revealed that, compared with in normal hepatic tissues without tumor cell injection, there was a marked increase in MVD in tumor tissue formed by HepG2 cells. However, *Plasmodium* infection notably reduced the MVD in tumor tissues (Fig. 3A). Western blot analysis of CD31 expression levels in tumor tissues demonstrated consistent results with the IHC staining (Fig. 3B). Furthermore, the results revealed that CD31 expression level in hepatic tissues was significantly increased after HepG2 cell injection compared with the sham group without tumor cell injection, whilst *Plasmodium* infection significantly suppressed its upregulation (Fig. 3B). Subsequently, the protein levels of HIF-1α, VEGFA and Ang2, which are implicated in angiogenesis, were assessed. The findings demonstrated that the protein levels of HIF-1α, VEGFA and Ang2 were significantly increased in both tumor and para-cancerous hepatic tissues when compared with hepatic tissues in the sham group. Infection of *Plasmodium* significantly reduced their expression in both tumor and para-cancerous tissues (Fig. 3C). Moreover, RT-qPCR analysis of MMP-2, MMP-9 and inflammatory cytokines (IL-1β, IL-6, TNF-α) also revealed that these genes were significantly upregulated in both tumor and para-cancerous tissues from the mice injected with HepG2 cells when compared with the sham group, whilst *Plasmodium* infection significantly reduced their expression in comparison with the group injected with HepG2 cells alone (Fig. 3D). These results indicate that *Plasmodium* suppresses neo-vascularization during tumorigenesis of liver cancer.

Plasmodium infection hinders the tumorigenesis of HepG2 cells by downregulating HIF-1α. To assess the role of HIF-1α in mediating the effect of *Plasmodium* infection on tumorigenesis, HepG2 cells or cells transduced with a lentivirus expressing HIF-1α were injected into the left liver lobe of nude mice in the presence or absence of *Plasmodium* infection. A total of three different clones of HepG2 cells transduced with HIF-1α expression lentivirus were initially generated, and clone 2, which demonstrated the highest HIF-1α expression, was used for subsequent liver injection (Fig. 4A). Western blot analysis of HIF-1α expression in the tumor tissues demonstrated that *Plasmodium* infection significantly reduced HIF-1α expression when compared with the uninfected group, and HIF-1α expression level was significantly restored in tumor tissues with lentivirus-mediated HIF-1α overexpression (Fig. 4B). However, HIF-1α expression remained at a low level in para-cancerous hepatic tissues upon *Plasmodium* infection, regardless of the overexpression of HIF-1α in tumor tissues. Giemsa staining revealed that infection of Py led to an equal level of hemozoin deposition in tumors with or without HIF-1α overexpression (Fig. 4C), indicating that HIF-1α expression level did not affect *Plasmodium* infection. However, restoration of HIF-1α expression in HepG2 cells significantly promoted tumor growth under the condition of *Plasmodium* infection compared with the group without ectopic HIF-1α overexpression (Fig. 4D and E). Furthermore, TUNEL staining in tumor sections revealed that *Plasmodium* infection significantly induced cell death in tumor tissues compared with the group without infection, and restoration of HIF-1α expression partially rescued this effect when compared with the group without ectopic HIF-1α overexpression (Fig. 4F). Together, the findings imply that suppression of HIF-1α expression contributes to the anti-tumorigenic effect of Py infection.

Plasmodium infection curbs angiogenesis in hepatic tumor development through targeting HIF-1α. The present study then evaluated whether HIF-1α expression regulates

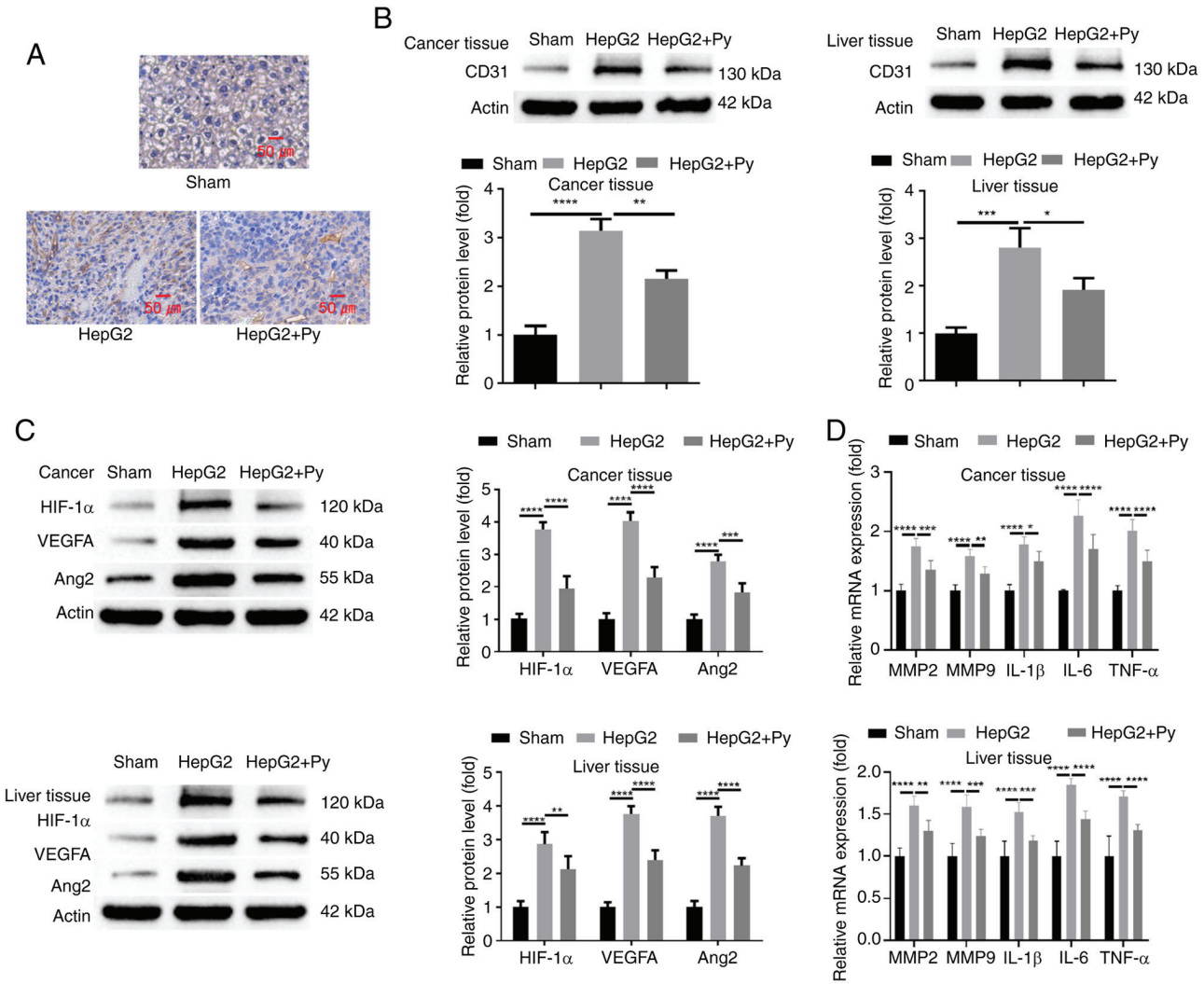

Figure 3. *Plasmodium* infection attenuates angiogenesis in hepatic tumor tissues and para-cancerous tissues. (A) Analysis of microvascular density by immunohistochemical staining of CD31 in normal hepatic tissues (sham group) and tumor tissues with or without Py infection (HepG2 + Py and HepG2 groups, respectively). Western blot analysis of (B) CD31 and (C) HIF-1α, VEGFA and Ang2 protein levels in normal hepatic tissues (sham group), and tumor and para-cancerous hepatic tissues with or without Py infection. (D) Reverse transcription-quantitative PCR analysis of MMP-2, MMP-9 and inflammatory cytokines (IL-1β, IL-6 TNF-α) in normal hepatic tissues (sham group), and tumor and para-cancerous hepatic tissues with or without Py infection. Tissues for analysis in the sham group were normal hepatic tissues without HepG2 cell injection. n=5 in each group. *P<0.05; **P<0.01; ***P<0.001; ****P<0.0001. Py, *Plasmodium yoelii*; HIF-1α, hypoxia-inducible factor 1α; VEGFA, vascular endothelial growth factor A; Ang2, angiopoietin 2; MMP, matrix metalloproteinase; IL, interleukin; TNF, tumor necrosis factor.

vascularization during hepatic tumor development upon Py infection. Analysis of MVD by anti-CD31 IHC staining revealed that *Plasmodium* infection markedly reduced the MVD in tumor tissues compared with the group without infection, whilst in the group with HIF-1α overexpression, the level of MVD was largely restored when compared with the group without ectopic HIF-1α overexpression (Fig. 5A). Western blot analysis of CD31 expression levels in tumor tissues of the different groups demonstrated consistent results with the IHC staining (Fig. 5B). Furthermore, the protein levels of angiogenic factors (VEGFA and Ang2), which were significantly suppressed upon infection with *Plasmodium* compared with the group without infection, were significantly increased after HIF-1α overexpression in the HepG2 cells (Fig. 5C). RT-qPCR analysis of MMP-2, MMP-9 and inflammatory cytokines (IL-1β, IL-6 TNF-α) also revealed that HIF-1α overexpression significantly reduced the suppressive effect of *Plasmodium* infection on their expression when compared with the group without ectopic HIF-1α overexpression (Fig. 5D). Together, these findings indicate that *Plasmodium* suppresses neo-vascularization during tumorigenesis of liver cancer through targeting HIF-1α.

Discussion

The present study demonstrated that *Plasmodium* infection could suppress tumorigenesis and vascularization in a mouse model of implanted HepG2 cells. *Plasmodium* infection suppressed the expression of pro-angiogenic factors (VEGFA and ANG2), MMP2, MMP9 and inflammatory cytokines (TNF-α, IL-6 and IL-1β), which are implicated in the angiogenesis and invasion of hepatic tumor cells (30-33). Moreover, the findings indicate that downregulation of

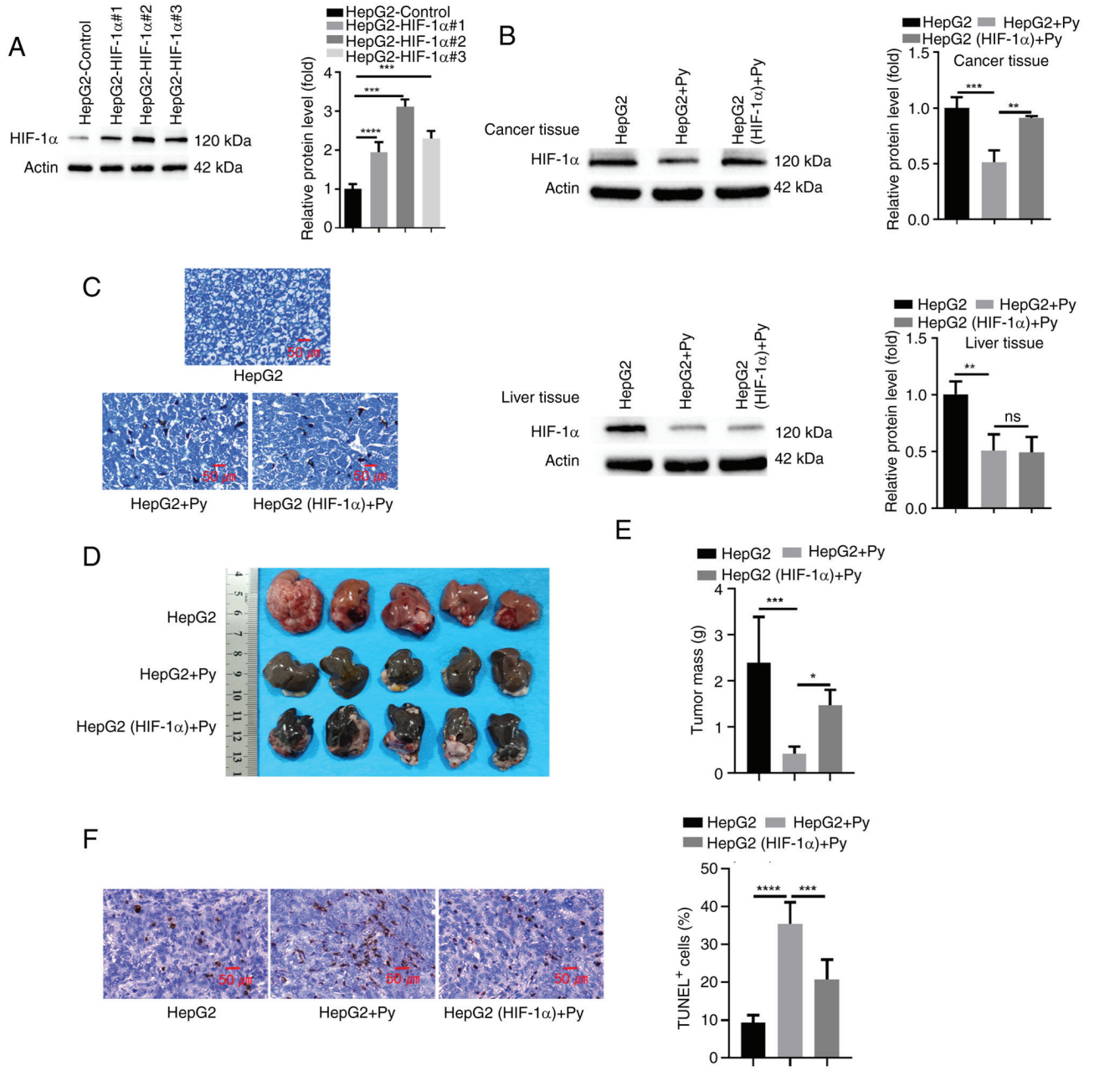

Figure 4. *Plasmodium* infection hinders the tumorigenesis of HepG2 cells by downregulating HIF-1α. (A) A total of three different clones of HepG2 cells transduced with HIF-1α expression lentivirus were analyzed using western blotting. Clone 2 demonstrated the highest HIF-1α expression and was therefore used for subsequent liver injection. HepG2 cells or cells transduced with a lentivirus expressing HIF-1α [Clone 2: HepG2 (HIF-1α)] were injected into the left liver lobe of nude mice in the presence or absence of *Plasmodium* infection. (B) Western blot analysis of HIF-1α expression in tumor tissues and para-cancerous hepatic tissues. (C) Giemsa staining of hemozoin in the tumor tissues. (D) Images of representative xenograft tumors in each experimental group. (E) Summary of tumor masses in each group. (F) Detection of apoptotic events by TUNEL staining. n=5 in each group. *P<0.05; **P<0.01; ***P<0.001; ****P<0.0001. Py, *Plasmodium yoelii*; HIF-1α, hypoxia-inducible factor 1α.

HIF-1α is associated with the anti-angiogenic effect of *Plasmodium* infection. The results of the present study also demonstrate that *Plasmodium* infection may be combined with anti-angiogenic agents to limit vascularization and progression of liver cancer.

After delivery to the blood by mosquitoes, *Plasmodium* parasites can inhabit hepatocytes in a dormant state or mature and reproduce in hepatocytes, which significantly alters the physiological features of liver tissues (34,35). The *Plasmodium berghei* NK65 strain has been reported to induce oxidative stress in mouse liver tissues and *Plasmodium chabaudi* infection can trigger liver inflammation, and increase production of serum liver enzymes (36,37). In addition, *Plasmodium falciparum* has been reported to promote anaerobic glycolysis in hepatocytes to produce lactic acid, which may be linked with the development of hypoglycemia and lactic acidosis (38).

Global epidemiological analysis has revealed that the worldwide malaria incidence is inversely associated with mortality in patients with solid cancer, including lung, breast, stomach and colon cancer (23). It has been well-documented that *Plasmodium* infection could exert an anticancer effect, especially in liver cancer (39). *Plasmodium* parasites could

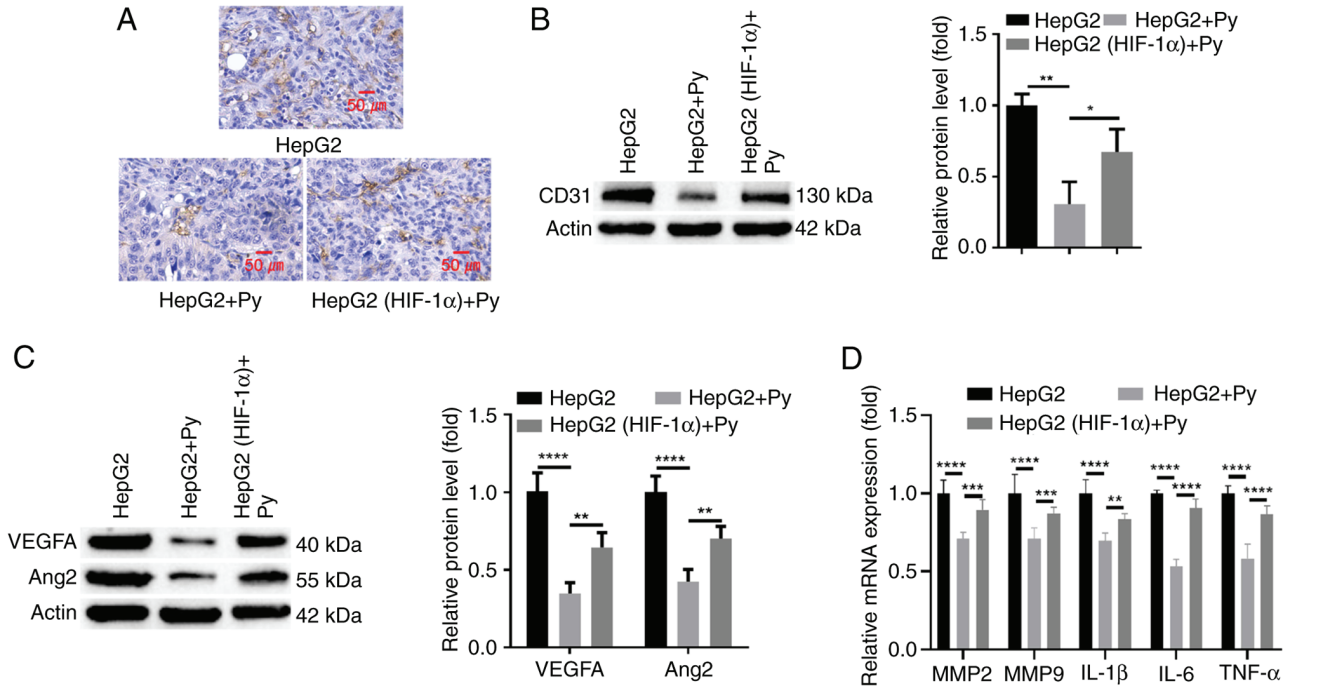

Figure 5. *Plasmodium* infection curbs angiogenesis during hepatic tumor development through targeting HIF-1α. HepG2 cells or cells transduced with a lentivirus expressing HIF-1α were injected into the left liver lobe of nude mice in the presence or absence of *Plasmodium* infection. (A) Analysis of microvascular density using immunohistochemical staining of CD31 in tumor tissue sections. Western blot analysis of (B) CD31 and (C) HIF-1α, VEGFA and Ang2 protein levels in tumor tissues. (D) Reverse transcription-quantitative PCR analysis of MMP-2, MMP-9 and inflammatory cytokines (IL-1β, IL-6 TNF-α) in tumor tissues. n=5 in each group. *P<0.05; **P<0.01; ***P<0.001; ****P<0.0001. Py, *Plasmodium yoelii*; HIF-1α, hypoxia-inducible factor 1α; VEGFA, vascular endothelial growth factor A; Ang2, angiopoietin 2; MMP, matrix metalloproteinase; IL, interleukin; TNF, tumor necrosis factor.

impinge on several regulatory pathways involved in cell survival, proliferation, autophagy and p53 signaling in liver cells (40), which may underlie the anti-tumorigenic effect. Furthermore, *Plasmodium* has been recognized as an immunomodulatory agent that boosts anticancer immunity (41). *Plasmodium* infection suppresses the release of cytokines and chemokines responsible for the recruitment of regulatory T cells and tumor-associated macrophages in tumor tissues, thus ameliorating the immunosuppressive tumor microenvironment (21,25). In addition, *Plasmodium* parasites have been reported to serve as a cancer vaccine to induce tumor antigen-specific T cell responses in a murine liver cancer model (42).

The results of the present study also support that *Plasmodium* infection could suppress tumorigenesis in a mouse model of implanted HepG2 cells. As a highly vascularized malignancy, neo-angiogenesis is critical for tumor growth and progression of liver cancer (31). The present study demonstrated that *Plasmodium* infection significantly suppressed angiogenesis in hepatic tumor tissues derived from HepG2 cells in nude mice, which may be a key factor limiting tumorigenesis of liver cancer cells upon *Plasmodium* infection. There are several lines of evidence supporting the anti-angiogenic effect of *Plasmodium* infection in liver cancer. *Plasmodium* infection could curb tumor angiogenesis by reducing infiltration of tumor-associated macrophages in a mouse model of implanted liver cancer cells (25). Furthermore, *Plasmodium* infection could modulate expression of microRNAs and long non-coding RNA (F66), which target the VEGF/VEGFR2 signaling pathway to limit angiogenesis (22,43).

The present study revealed that *Plasmodium* infection reduced the expression levels of HIF-1α in hepatic tumors, and HIF-1α overexpression restored angiogenesis and tumor growth under the condition of *Plasmodium* infection. Hypoxia is a key hallmark of the tumor microenvironment, which leads to the activation of hypoxia-induced gene expression and responses by stabilizing HIF-1α (44). Activation of HIF-1α signaling has a significant impact on cancer cell metabolism, but also impinges on vasculature formation (45). In both physiological and pathophysiological conditions, HIF-1α serves as a master regulator of angiogenesis by upregulating pro-angiogenic factors such as VEGFs (46). The extracellular matrix remodeling factors (such as MMP-2 and MMP-9) are also transcriptional targets of HIF-1α (47,48). Moreover, high HIF-1α expression is associated with a poor prognosis in patients with liver cancer (49), and activation of the hypoxic signaling pathway is closely associated with poor prognosis in patients with liver cancer (50,51). Therefore, the findings of the present study suggest that *Plasmodium* infection could restrain angiogenesis in liver cancer by curtailing HIF-1α expression. Suppressed angiogenesis may impair nutrient and oxygen supply to developing tumor tissues and hinder local invasion of cancerous cells. Future work is warranted to further dissect the mechanisms by which *Plasmodium* infection attenuates HIF-1α expression in liver cancer.

The current study presents intriguing findings that *Plasmodium* infection can suppress tumor growth and angiogenesis in a mouse model of liver cancer, potentially through downregulation of HIF-1α. However, the use of an immunodeficient mouse model, the lack of evidence for specific

targeting of tumor cells without affecting normal tissues, the incomplete understanding of the underlying mechanisms, and the uncertain translational potential to human malaria parasites limit the current clinical applicability. Addressing these limitations through further research using immunocompetent models of hepatic cancer, comprehensive toxicity analyses, mechanistic studies, and exploration of attenuated or inactivated parasite forms is crucial to assess the feasibility and safety of potential *Plasmodium*-based anticancer interventions. Furthermore, although the gene expression of MMP9, MMP8, IL-1B and IL-6 were analyzed in the present study, these factors were not evaluated at the protein level, which could provide additional insights into their functional roles in the observed effect.

In conclusion, the present study demonstrated the anti-angiogenic and anti-tumorigenic effects of *Plasmodium* infection in a mouse model of implanted HepG2 cells. Reduced HIF-1α expression in hepatic tumor tissues may account for the anti-angiogenic effect of *Plasmodium* infection. Furthermore, *Plasmodium* parasites may be used jointly with other anti-angiogenic agents to limit neo-vascularization in liver cancer treatment.

Acknowledgements

Not applicable.

Funding

The present work was supported by the Yunnan Health Training Project of High Level Talents (grant no. H-2019039).

Availability of data and materials

The data generated in the present study may be requested from the corresponding author.

Authors' contributions

YL conceived and designed the study. HC, ML, RW and XC were responsible for data collection. ML, RW and XC performed the analysis and interpretation of results. RW, XC and YL prepared the draft manuscript. RW, XC and YL confirm the authenticity of all the raw data. All authors read and approved the final version of the manuscript.

Ethics approval and consent to participate

The animal protocols in the present study were approved by the Experimental Animal Ethics Committee of Yunnan Bestai Biotechnology Co (Kunming, China; approval no. BST-MICE-20221229-01).

Patient consent for publication

Not applicable.

Competing interests

The authors declare that they have no competing interests.

References

1. Oh JH and Jun DW: The latest global burden of liver cancer: A past and present threat. Clin Mol Hepatol 29: 355-357, 2023.
2. Llovet JM, Kelley RK, Villanueva A, Singal AG, Pikarsky E, Roayaie S, Lencioni R, Koike K, Zucman-Rossi J, Finn RS: Hepatocellular carcinoma. Nat Rev Dis Primers 7: 6, 2021.
3. Gilles H, Garbutt T and Landrum J: Hepatocellular Carcinoma. Crit Care Nurs Clin North Am 34: 289-301, 2022.
4. Ganesan P and Kulik LM: Hepatocellular carcinoma: New developments. Clin Liver Dis 27: 85-102, 2023.
5. Siegel AB and Zhu AX: Metabolic syndrome and hepatocellular carcinoma: Two growing epidemics with a potential link. Cancer 115: 5651-5661, 2009.
6. Jiang Y, Han Q, Zhao H and Zhang J: The Mechanisms of HBV-Induced Hepatocellular Carcinoma. J Hepatocell Carcinoma 8: 435-450, 2021.
7. Powell EE, Wong VW and Rinella M: Non-alcoholic fatty liver disease. Lancet 397: 2212-2224, 2021.
8. Wen T, Jin C, Facciorusso A, Donadon M, Han HS, Mao Y, Dai C, Cheng S, Zhang B, Peng B, *et al*: Multidisciplinary management of recurrent and metastatic hepatocellular carcinoma after resection: An international expert consensus. Hepatobiliary Surg Nutr 7: 353-371, 2018.
9. Bray F, Ferlay J, Soerjomataram I, Siegel RL, Torre LA and Jemal A: Global cancer statistics 2018: GLOBOCAN estimates of incidence and mortality worldwide for 36 cancers in 185 countries. CA Cancer J Clin 68: 394-424, 2018.
10. Lee JC, Hung HC, Wang YC, Cheng CH, Wu TH, Lee CF, Wu TJ, Chou HS, Chan KM and Lee WC: Risk score model for microvascular invasion in hepatocellular carcinoma: The Role of tumor burden and alpha-fetoprotein. Cancers (Basel) 13: 4403, 2021.
11. Morse MA, Sun W, Kim R, He AR, Abada PB, Mynderse M and Finn RS: The role of angiogenesis in hepatocellular carcinoma. Clin Cancer Res 25: 912-920, 2019.
12. Moawad AW, Szklaruk J, Lall C, Blair KJ, Kaseb AO, Kamath A, Rohren SA and Elsayes KM: Angiogenesis in hepatocellular carcinoma; pathophysiology, targeted therapy, and role of imaging. J Hepatocell Carcinoma 7: 77-89, 2020.
13. Pinto E, Pelizzaro F, Farinati F and Russo FP: Angiogenesis and hepatocellular carcinoma: From molecular mechanisms to systemic therapies. Medicina (Kaunas) 59: 1115, 2023.
14. Deryugina EI and Quigley JP: Tumor angiogenesis: MMP-mediated induction of intravasation- and metastasis-sustaining neovasculature. Matrix Biol 44-46: 94-112, 2015.
15. Geervliet E and Bansal R: Matrix Metalloproteinases as potential biomarkers and therapeutic targets in liver diseases. Cells 9: 1212, 2020.
16. Hammam O, Mahmoud O, Zahran M, Sayed A, Salama R, Hosny K and Farghly A: A possible role for TNF-α in coordinating inflammation and angiogenesis in chronic liver disease and hepatocellular carcinoma. Gastrointest Cancer Res 6: 107-114, 2013.
17. Pocino K, Stefanile A, Basile V, Napodano C, D'Ambrosio F, Di Santo R, Callà CAM, Gulli F, Saporito R, Ciasca G, *et al*: Cytokines and hepatocellular carcinoma: biomarkers of a deadly embrace. J Pers Med 13: 5, 2022.
18. Tak KH, Yu GI, Lee MY and Shin DH: Association between polymorphisms of interleukin 1 family genes and hepatocellular carcinoma. Med Sci Monit 24: 3488-3495, 2018.
19. Zhu AX, Duda DG, Sahani DV and Jain RK: HCC and angiogenesis: Possible targets and future directions. Nat Rev Clin Oncol 8: 292-301, 2011.
20. Tavares J, Formaglio P, Thiberge S, Mordelet E, Van Rooijen N, Medvinsky A, Ménard R and Amino R: Role of host cell traversal by the malaria sporozoite during liver infection. J Exp Med 210: 905-915, 2013.
21. Adah D, Yang Y, Liu Q, Gadidasu K, Tao Z, Yu S, Dai L, Li X, Zhao S, Qin L, *et al*: Plasmodium infection inhibits the expansion and activation of MDSCs and Tregs in the tumor microenvironment in a murine Lewis lung cancer model. Cell Commun Signal 17: 32, 2019.
22. Yang Y, Liu Q, Lu J, Adah D, Yu S, Zhao S, Yao Y, Qin L, Qin L and Chen X: Exosomes from Plasmodium-infected hosts inhibit tumor angiogenesis in a murine Lewis lung cancer model. Oncogenesis 6: e351, 2017.

23. Qin L, Chen C, Chen L, Xue R, Ou-Yang M, Zhou C, Zhao S, He Z, Xia Y, He J, *et al*: Worldwide malaria incidence and cancer mortality are inversely associated. Infect Agent Cancer 12: 14, 2017.
24. Liang Y, Chen X, Tao Z, Ma M, Adah D, Li X, Dai L, Ding W, Fanuel S, Zhao S, *et al*: Plasmodium infection prevents recurrence and metastasis of hepatocellular carcinoma possibly via inhibition of the epithelial-mesenchymal transition. Mol Med Rep 23: 418, 2021.
25. Wang B, Li Q, Wang J, Zhao S, Nashun B, Qin L and Chen X: Plasmodium infection inhibits tumor angiogenesis through effects on tumor-associated macrophages in a murine implanted hepatoma model. Cell Commun Signal 18: 157, 2020.
26. Blidisel A, Marcovici I, Coricovac D, Hut F, Dehelean CA and Cretu OM: Experimental models of hepatocellular carcinoma-a preclinical perspective. Cancers (Basel) 13: 3651, 2021.
27. Li J, Wang X, Ren M, He S and Zhao Y: Advances in experimental animal models of hepatocellular carcinoma. Cancer Med 12: 15261-15276, 2023.
28. Liu S, Huang F, Ru G, Wang Y, Zhang B, Chen X and Chu L: Mouse models of hepatocellular carcinoma: Classification, advancement, and application. Front Oncol 12: 902820, 2022.
29. Livak KJ and Schmittgen TD: Analysis of relative gene expression data using real-time quantitative PCR and the 2(-Delta Delta C(T)) Method. Methods 25: 402-408, 2001.
30. Yang YM, Kim SY and Seki E: Inflammation and liver cancer: Molecular mechanisms and therapeutic targets. Semin Liver Dis 39: 26-42, 2019.
31. Yao C, Wu S, Kong J, Sun Y, Bai Y, Zhu R, Li Z, Sun W and Zheng L: Angiogenesis in hepatocellular carcinoma: Mechanisms and anti-angiogenic therapies. Cancer Biol Med 20: 25-43, 2023.
32. Sanz-Cameno P, Trapero-Marugán M, Chaparro M, Jones EA and Moreno-Otero R: Angiogenesis: From chronic liver inflammation to hepatocellular carcinoma. J Oncol 2010: 272170, 2010.
33. Quintero-Fabián S, Arreola R, Becerril-Villanueva E, Torres-Romero JC, Arana-Argáez V, Lara-Riegos J, Ramírez-Camacho MA and Alvarez-Sánchez ME: Role of Matrix Metalloproteinases in Angiogenesis and Cancer. Front Oncol 9: 1370, 2019.
34. Kluck GEG, Wendt CHC, Imperio GED, Araujo MFC, Atella TC, da Rocha I, Miranda KR and Atella GC: Plasmodium infection induces dyslipidemia and a hepatic lipogenic state in the host through the inhibition of the AMPK-ACC pathway. Sci Rep 9: 14695, 2019.
35. Balasubramanian L, Zuzarte-Luís V, Syed T, Mullick D, Deb S, Ranga-Prasad H, Meissner J, Almeida A, Furstenhaupt T, Siddiqi K, *et al*: Association of plasmodium berghei with the apical domain of hepatocytes is necessary for the parasite's liver stage development. Front Cell Infect Microbiol 9: 451, 2020.
36. Scaccabarozzi D, Deroost K, Corbett Y, Lays N, Corsetto P, Salè FO, Van den Steen PE and Taramelli D: Differential induction of malaria liver pathology in mice infected with Plasmodium chabaudi AS or Plasmodium berghei NK65. Malar J 17: 18, 2018.
37. Deroost K, Lays N, Pham TT, Baci D, Van den Eynde K, Komuta M, Prato M, Roskams T, Schwarzer E, Opdenakker G and Van den Steen PE: Hemozoin induces hepatic inflammation in mice and is differentially associated with liver pathology depending on the Plasmodium strain. PLoS One 9: e113519, 2014.
38. Daily JP, Scanfeld D, Pochet N, Le Roch K, Plouffe D, Kamal M, Sarr O, Mboup S, Ndir O, Wypij D, *et al*: Distinct physiological states of Plasmodium falciparum in malaria-infected patients. Nature 450: 1091-1095, 2017.
39. Ding H, Wu S, Jin Z, Zheng B, Hu Y, He K, Lu S and Zhuo X: Anti-Tumor effect of parasitic protozoans. Bioengineering (Basel) 9: 395, 2022.
40. Kaushansky A, Ye AS, Austin LS, Mikolajczak SA, Vaughan AM, Camargo N, Metzger PG, Douglass AN, MacBeath G and Kappe SH: Suppression of host p53 is critical for Plasmodium liver-stage infection. Cell Rep 3: 630-637, 2013.
41. Chen X, Qin L, Hu W and Adah D: The mechanisms of action of Plasmodium infection against cancer. Cell Commun Signal 19: 74, 2021.
42. Liu Q, Yang Y, Tan X, Tao Z, Adah D, Yu S, Lu J, Zhao S, Qin L, Qin L and Chen X: Plasmodium parasite as an effective hepatocellular carcinoma antigen glypican-3 delivery vector. Oncotarget 8: 24785-24796, 2017.
43. Qin L, Zhong M, Adah D, Qin L, Chen X, Ma C, Fu Q, Zhu X, Li Z, Wang N and Chen Y: A novel tumour suppressor lncRNA F630028O10Rik inhibits lung cancer angiogenesis by regulating miR-223-3p. J Cell Mol Med 24: 3549-3559, 2020.
44. Jun JC, Rathore A, Younas H, Gilkes D and Polotsky VY: Hypoxia-Inducible Factors and Cancer. Curr Sleep Med Rep 3: 1-10, 2017.
45. Kierans SJ and Taylor CT: Regulation of glycolysis by the hypoxia-inducible factor (HIF): Implications for cellular physiology. J Physiol 599: 23-37, 2021.
46. Lv X, Li J, Zhang C, Hu T, Li S, He S, Yan H, Tan Y, Lei M, Wen M and Zuo J: The role of hypoxia-inducible factors in tumor angiogenesis and cell metabolism. Genes Dis 4: 19-24, 2016.
47. Manuelli V, Pecorari C, Filomeni G and Zito E: Regulation of redox signaling in HIF-1-dependent tumor angiogenesis. FEBS J 289: 5413-5425, 2022.
48. Zhao L, Liu Z, Yang F, Zhang Y, Xue Y, Miao H, Liao X, Huang H and Li G: Intrabody against prolyl hydroxylase 2 promotes angiogenesis by stabilizing hypoxia-inducible factor-1α. Sci Rep 9: 11861, 2019.
49. Zheng SS, Chen XH, Yin X and Zhang BH: Prognostic significance of HIF-1α expression in hepatocellular carcinoma: A meta-analysis. PLoS One 8: e65753, 2013.
50. Li Q, Jin L and Jin M: Novel hypoxia-related gene signature for risk stratification and prognosis in hepatocellular carcinoma. Front Genet 12: 613890, 2021.
51. Deng F, Chen D, Wei X, Lu S, Luo X, He J, Liu J, Meng T, Yang A and Chen H: Development and validation of a prognostic classifier based on HIF-1 signaling for hepatocellular carcinoma. Aging (Albany NY) 12: 3431-3450, 2020.

Copyright © 2024 Wu et al. This work is licensed under a Creative Commons Attribution-NonCommercial-NoDerivatives 4.0 International (CC BY-NC-ND 4.0) License.